Active Polarization Modulation of Terahertz Radiation Using Metamaterial/Graphene-Based Optoelectronic Devices

Abdullah M. Zaman[1,2], Yuezhen Lu[1], Nikita W. Almond[3], Oliver J. Burton[4], Jack Alexander-Webber[4], Stephan Hofmann[4], Thomas Mitchell[3], Jonathan D. P. Griffiths[3], Harvey E. Beere[3], David A. Ritchie[3], and Riccardo Degl'Innocenti[1]

[1]School of Engineering, University of Lancaster, Bailrigg, Lancaster LA1 4YW, United Kingdom
[2] College of Engineering, Taibah University, Madina 42353, Saudi Arabia
[3]Cavendish Laboratory, University of Cambridge, J J Thomson Avenue, Cambridge CB3 0HE, United Kingdom
[4]Department of Engineering, University of Cambridge, 9 J. J. Thomson Avenue, Cambridge CB3 0FA, United Kingdom

***Abstract*—We investigate the modulation performance of a metamaterial/graphene optoelectronic device in the THz range. Operating characteristics such as amplitude, phase and polarization modulations of broadband THz radiation are reported. The accomplishments of modulation depth include >75% in spectral amplitude, >15º in spectral phase, >0.2 active modulation of ellipticity ratio, and active rotational angle changes of 20º. These achievements are the key elements towards efficient manipulations of THz radiation for applications such as next-generation wireless communications, spectroscopy, and imaging.**

I. Introduction

RESEARCH in the terahertz (THz) band, which generally covers the whole spectrum between 0.1-10 THz, is rapidly increasing to fulfil the needs for high-speed data transmission in communications, spectroscopy and imaging [1-2]. Approaches from all-electronics encounter significant efficiency drop beyond 500 GHz, despite the progress achieved at 300 GHz with CMOS technology [3]. Thus, approaches different from all-electronics need to be developed in light of the inevitable expansion of few applications, mostly wireless communications, towards the high frequency THz spectrum. Therefore, approaches based on photonic aspects have been targeted towards the development of fast, external optoelectronic modulators [4]. Due to versatility, power efficiency, small footprint, and their integration capabilities, metamaterials (MMs) loaded with graphene as an active element have been extensively used to achieve dynamic modulation in the THz band [4]. Nested metamaterial array modulator was designed achieving 1 GHz of modulation bandwidth [5] using 2DEG as tuneable material. Metallic bow-tie antennas shunted by graphene were demonstrated to operate with a modulation speed >115 MHz [6].

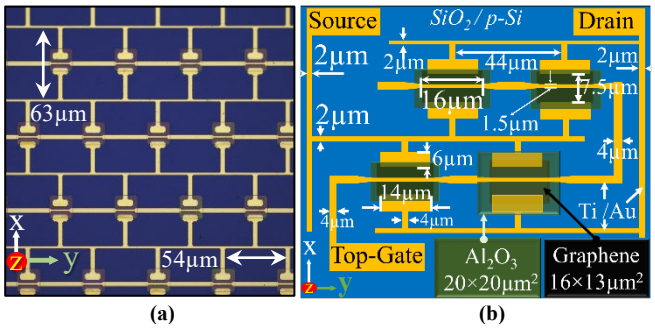

(a) (b)

Fig. 1. (a) An optical microscope picture of a complete array of the fabricated gated/SRRs; (b) schematic top-view of the gated MM/graphene array fabricated on top of a SiO_2/p-doped silicon substrate to allow for back-gating.

AZ, YL and RD acknowledge support from EPSRC, (Grant No. EP/S019383/1)

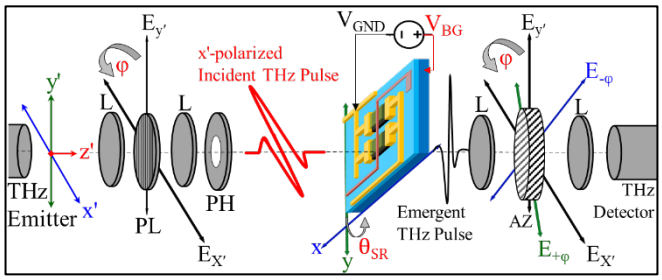

Fig. 2. Schematic view of the terahertz time-domain spectroscopy (THz-TDS) experimental setup to acquire the temporal pulses of a THz source. L: lenses, PL: polarizer, φ: polarizer's and analyzer's angles with respect to y'-axis, PH: pinhole (iris), Θ_{SR}: split-resonators angle with respect to x'-axis, V_{GND}: source/drain voltage, V_{BG}: backgate voltage, and AZ: analyzer

Here we report an engineered design of MMs/graphene gated split-ring resonators (gated/SRRs) operating at 0.8 THz capable of dynamically modify the spectral amplitude by >75% at resonance. Spectral relative phase changes are exceeding 15º for 0.68 THz. In [7], the polarization modulation was achieved by using an electromagnetically induced transparency (EIT) technique whereas in [8], a MM/graphene double layer of polarization device was fabricated to yield an artificial chiral response. Here, we basically exploit the strong amplitude and phase anisotropy of this new architecture to achieve an ellipticity modulation of >0.2 and a dynamic rotation of the polarization plane by >20º at 0.66 THz by using a classic crossed polarizer scheme. It is worth mentioning that these values are calculated by using temporal resolved measurements and considering all the entire transmitted time waveform including Fabry-Perot resonances as in [9]. Significantly, similar polarization modulation performances are achieved with GHz instead of MHz reconfiguration speed. These results represent great potential towards fast and robustness of THz modulators for communications beyond 5G or holography.

II. Structure and Experimental Setup

The novel design and development of the engineered gated/SRRs with MMs/graphene are reported previously in [10], [11]. The fabricated device consists of 22 × 20 SRRs array arranged in an interdigitated scheme as shown in Fig. 1(a). The single unit-cell layers including the active element (graphene) and the dielectric layer (Al_2O_3) are shown in Fig. 1(b). The device is tested in the THz time-domain spectroscopy (THz-TDS) setup, from Menlo Systems model Tera K15, with the addition of two polarizers as illustrated in Fig. 2. Both the THz emitter and detector are kept at the horizontal polarization state, while the first polarizer is set to the full transmission angle(φ_{PL}=

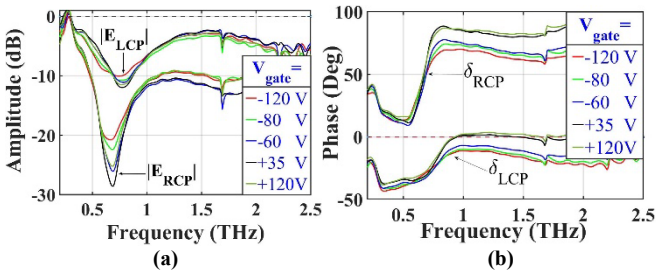

Fig. 3. Circular transmission coefficients of the E-field spectral amplitudes (a) and relative phases (b).

90°). The device is rotated by Θ_{SR}= 45° in order to divide the incident horizontally polarized E-field into two orthogonal components with respect to the resonators' plane of incident (i.e. $E_{\pm45^o}$). The backgate voltage (V_{BG}) is gradually swept from -120 V to +120 V by connecting it to the positive terminal of a source-meter-unit (SMU), from Kethley model 2450, while grounding the source/drain pads (V_{GND}). The transmitted E-field is then recorded at different backgate voltages.

III. Results and Discussion

The manipulation of polarization states was conducted to investigate the optical activity (OA) and circular dichroism (CD) of the device. The linear transmission coefficients ($A_{\pm45^o}$ amplitudes and phases) are acquired by rotating the analyzer's angle at $\phi = \pm45^o$ to selectively detect the transmitted E-fields along the x or y directions. The linear transmission coefficients ($A_{\pm45^o}$) are converted into circular (E_{RCP} and E_{LCP}, right and left hand polarization components of the E-field, respectively) via the formalism described in [11] as follows:

$$\begin{pmatrix} E_{RCP}(\omega) \\ E_{LCP}(\omega) \end{pmatrix} = \frac{1}{\sqrt{2}} \begin{pmatrix} 1 & i \\ 1 & -i \end{pmatrix} \begin{pmatrix} E_{+45^o}(\omega) \\ E_{-45^o}(\omega) \end{pmatrix} = \frac{1}{\sqrt{2}} \begin{pmatrix} 1 & i \\ 1 & -i \end{pmatrix} \begin{pmatrix} |A_{+45^o}(\omega)| e^{i\delta_{+45^o}(\omega)} \\ |A_{-45^o}(\omega)| e^{i\delta_{-45^o}(\omega)} \end{pmatrix} \quad (1)$$

Where $A_{\pm45^o}$ and $\delta_{\pm45^o}$ are the spectral amplitudes and phases of the detected E-fields after rotating the analyzer's angle by φ_{AZ}= ±45°, respectively. Extinction ratio of >6 dB is reported for the spectral amplitudes of $|E_{RCP}|$ as shown in Fig. 3(a) at resonance, hence achieving a dynamic manipulation of the polarization state. Moreover, >15° in the spectral relative phases is observed for 0.68 THz as plotted in Fig. 3(b). These values were calculated by including in the post-processing of the circular $E_{\pm45^o}$-fields only the first transmitted temporal pulses as described in [10], [11].

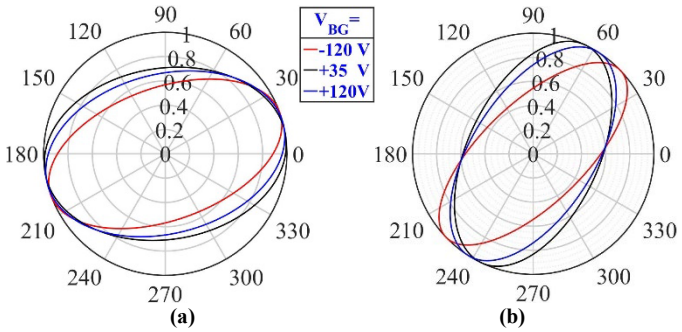

Fig. 4. (a) 0.66 THz and (b) 0.73 THz states of polarization.

The OA and CD were calculated using the formulas for Ψ and η, respectively, as described in [11]. Considerations of all the emergent temporal pulses during post-processing processing is approximating the results achievable by using a continues wave (CW) source. By including all the pulses in the time waveform, this modulator yielded ΔΨ= 20° for 0.66 THz with an ellipticity ratio change between 0.8 to 0.6 as shown by the polarization ellipses in Fig. 4(a). Moreover, the ellipticity ratio is reduced by Δη >0.2 (from ~0.6 to ~0.4) for 0.73 THz as shown by the ellipses plotted in Fig. 4(b). The ellipses were calculated by solving the quadratic equations as described in [11], [12] in the polar coordinates as follows:

$$\frac{E_x^2}{|A_{+45^o}|} - \frac{2E_xE_y\cos\Delta\delta}{|A_{+45^o}||A_{-45^o}|} + \frac{E_y^2}{|A_{-45^o}|} = \sin^2\Delta\delta \quad (2)$$

Where $\Delta\delta = \delta_{+45^o} - \delta_{-45^o}$. The E-field magnitudes were normalized to their maximum values before plotting the ellipses as illustrated in Fig. 4.

IV. Conclusion

In conclusion, we report on the realization of a fast, active modulator based on gated SRR array shunted by graphene operating in the THz range. The device achieved remarkable performances as an amplitude, phase, or polarization modulator depending on the experimental configuration. Amplitude modulation depth exceeded >6 dB with >15° of active phase modification when considering only the first transmitted pulse. By consideration of all temporal pulses, the depth of amplitude and phase modulations increase to >7.3 dB and >19°, respectively. As a polarization modulator, an active tuning of the OA was achieved by ΔΨ >20° at 0.66 THz. Similarly, an ellipticity modulation >0.2 was recorded at 0.73 THz. These high performances which have been achieved with >3 GHz reconfiguration speed, represent a fundamental step towards the realization of a fast, external optoelectronic platform in the THz range, for next generation wireless communication, imaging and spectroscopy.

References

[1] T. Nagatsuma, G. Ducournau, and C. C. Renaud, "Advances in terahertz communications accelerated by photonics," *Nat. Photon*., vol. 10, no. 6, pp. 371–379, May, 2016, doi: 10.1038/nphoton.2016.65.

[2] R. Degl'Innocenti, H. Lin, and M. Navarro-Cía, "Recent progress in terahertz metamaterial modulators," *Nanophotonics*, vol. 11, no. 8, 2022, pp. 1485-1514, doi: https://doi.org/10.1515/nanoph-2021-0803.

[3] S. Venkatesh, X. Lu, H. Saeidi, and K. Sengupta, "A high-speed programmable and scalable terahertz holographic metasurface based on tiled CMOS chips," *Nat. Electron*, vol. 3, no. 12, pp. 785–793, Dec., 2020, doi: https://doi.org/10.1038/s41928-020-00497-2

[4] S. Shen, X. Liu, Y. Shen, J. Qu, E. Pickwell-MacPherson, and X. Wei, "Recent Advances in the Development of Materials for Terahertz Metamaterial Sensing, " *Adv. Optical Mater.,* vol. 10, no. 1, pp. 2195-1071, Oct., 2022, doi: https://doi.org/10.1002/adom.202101008.

[5] Y. Zhao, L. Wang, Y. Zhang, S. Qiao, S. Liang, T. Zhou, X. Zhang, X. Guo, Z. Feng, F. Lan, Z. Chen, X. Yang, and Z. Yang, "High-speed efficient terahertz modulation based on tunable collective-individual state conversion within an active 3 nm two-dimensional electron gas metasurface," *Nano Lett.*, vol. 19, no. 11, pp. 7588–7597, Aug., 2019, doi: https://doi.org/10.1021/acs.nanolett.9b01273.

[6] D. S. Jessop, S. J. Kindness, L. Xiao, P. Braeuninger-Weimer, H. Lin, Y. Ren, C. X. Ren, S. Hofmann, J. A. Zeitler, H. E. Beere, D. A. Ritchie, and R. Degl'Innocenti, "Graphene based plasmonic terahertz amplitude modulator

operating above 100 MHz," *Appl. Phys. Lett.*, vol. 108, no. 147, pp. 171101, Apr., 2016, doi: https://doi.org/10.1063/1.4947596.
[7] S. J. Kindness, N. W. Almond, W. Michailow, B. Wei, L. A. Jakob, K. Delfanazari, P. Braeuninger-Weimer, S. Hofmann, H. E. Beere, D. A. Ritchie, and R. Degl'Innocenti, "Graphene-integrated metamaterial device for all-electrical polarization control of terahertz quantum cascade lasers," *ACS Photonics*, vol. 6, no. 6, pp. 1547–1555, May, 2019, doi: https://doi.org/10.1021/acsphotonics.9b00411.
[8] S. J. Kindness, N. W. Almond, W. Michailow, B. Wei, K. Delfanazari, P. Braeuninger-Weimer, S. Hofmann, H. E. Beere, D. A. Ritchie, and R. Degl'Innocenti, "A terahertz chiral metamaterial modulator," *Adv. Optical Mater.,* vol. 8, no. 21, pp. 2000581, Aug., 2020, doi: https://doi.org/10.1002/adom.202000581.
[9] R. Degl'Innocenti, S. J. Kindness, N. W. Almond, W. Michailow, P. Braeuninger-Weimer, S. Hofmann, H. E. Beere, and D. A. Ritchie, "Metamaterial/graphene active terahertz modulators," 2019 *IEEE MTT-S International Wireless Symposium (IWS)*, pp. 1–3, May 19-22, 2019, doi: 10.1109/IEEE-IWS.2019.8803931.
[10] A. M. Zaman, N. W. Almond, Y. Lu, X. Romain, D. De Lima, H. Lin, O. J. Burton, J. Alexander-Webber, S. Hofmann, T. Mitchell, J. D. P. Griffiths, H. E. Beere, D. A. Ritchie, and R. Degl'Innocenti, "Graphene-based External Optoelectronic Terahertz Modulators for High Speed Wireless Communications, " *14th UK-Europe-China Workshop on Millimetre-Waves and Terahertz Technologies (UCMMT)*, pp. 1-3, Sept. 13-15, 2021, doi: 10.1109/UCMMT53364.2021.9569931.
[11] A. M. Zaman, Y. Lu, X. Romain, N. W. Almond, O. J. Burton, J. Alexander-Webber, S. Hofmann, T. Mitchell, J. D. P. Griffiths, Harvey E. Beere, D. A. Ritchie, and R. Degl'Innocenti, "Terahertz Metamaterial Optoelectronic Modulators with GHz Reconfiguration Speed," in *IEEE Transactions on Terahertz Science and Technology*, vol. 3, no. 5, pp. 1-7, May, 2022, doi: 10.1109/TTHZ.2022.3178875.
[12] Y. Ji, F. Fan, S. Xu, J. Yu, and S. Chang, "Manipulation enhancement of terahertz liquid crystal phase shifter magnetically induced by ferromagnetic nanoparticles," *Nanoscale*, vol. 11, no. 11, pp. 4933–4941, Feb., 2019, doi: 10.1039/C8NR09259A